Available online at www.sciencedirect.com
SCIENCE DIRECT®
Journal of Nuclear Materials 327 (2004) 130–139
journal of nuclear materials
www.elsevier.com/locate/jnucmat

A critical test of the classical rate theory for void swelling

T. Okita *, W.G. Wolfer

Lawrence Livermore National Laboratory, 7000 East Ave., P.O. Box 808, Livermore, CA 94550-0808, USA

Received 9 July 2003; accepted 29 January 2004

Abstract

Complete sets of microstructural data have recently become available for two different irradiation times and for pure ternary alloys of austenitic stainless steels. Using these data as input to the classical rate theory of void swelling, swelling rates are computed and compared with the experimental data. Computations are performed for the ranges of physical parameters as suggested by experimental measurements or basic theory. It is found that classical rate theory predicts swelling rates in remarkably good agreement with the data for a limited set of parameter values. For example, dislocation bias factor ratios can be narrowed from the initial range of 1.1–2.0 down to the range of 1.25–1.55. An explanation is provided for the success of classical rate theory in spite of the fact that a significant fraction of interstitials form and migrate as clusters.

1. Introduction

The classical rate theory for void swelling was first developed by Harkness and Li [1], Brailsford and Bullough [2], and by Wiedersich [3] shortly after this phenomenon had been discovered in steels exposed to neutron irradiation in fast reactors. In this theory it was assumed that only mono-vacancies and self-interstitials are mobile defects of significant abundance. Small defect clusters were presumed to be present as the nuclei for voids or loops, and these nuclei were considered as stable, sessile sinks. With these assumptions, only three types of reactions needed to be considered, namely recombination between vacancies and interstitials, migration to and absorption at sinks, and thermal emission of vacancies from the various sinks. All three types of reactions can be derived from simple diffusion models.

The early predictions of the classical rate theory for void swelling beyond the low fluence data were disturbing as swelling accelerated with fluence. However, later on it was found [4] that swelling became eventually linear in fluence after a prolonged incubation period. During this non-linear incubation, a complex evolution takes place of the dislocation microstructure, of nucleation and disappearance of new voids, and simultaneously, of radiation-induced segregation of minor alloying elements into a precipitate microstructure different from the initial one. It is not surprising that this relatively simple classical rate theory could not do justice to all the complex evolutionary processes occurring concurrently and influencing each other.

Therefore, to conduct a fair test of the classical rate theory, two requirements must be met. First, pure metals or simple alloys without precipitates or secondary phases must be irradiated, and second, lacking reliable and tested models for void nucleation and for the evolution of dislocation microstructure, void concentrations and dislocation densities must be measured on irradiated specimens. Using this information, one can then compute the rate of void swelling at the doses for which a complete set of microstructure data exists. In a sense, one can compute and test the derivative of void swelling but not the integrated curve. This is the underlying concept for the present investigation.

We made use of the measured values of void swelling and the corresponding microstuctural data obtained by

* Corresponding author. Tel.: +1-925 422 5909; fax: +1-925 423 0785.
E-mail address: okita1@llnl.gov (T. Okita).

0022-3115/$ - see front matter © 2004 Elsevier B.V. All rights reserved.
doi:10.1016/j.jnucmat.2004.01.026

Okita et al. [5] for a pure ternary alloy irradiated at different neutron dose rates. For each condition of irradiation, two irradiation doses were obtained.

On the theory side, we review below the parameters necessary for rate theory calculations, and give ranges of acceptable values based on available data or fundamental theoretical derivations. We then seek sets of parameter values within the allowable parameter space which results in swelling rates most compatible with the experimentally observed trends. If no values can be found, it would indicate that classical rate theory is not adequate.

The objectives of this investigation are then to first explore what is needed in terms of future theoretical developments to go beyond the classical rate theory of void swelling. Second, several extensions have been proposed and examined to some degree in the past, such as production bias, production and one-dimensional motion of interstitial clusters, and enhanced recombination at centers. While these extensions are based on sound physical mechanisms, their significance relative to the basic mechanisms of the classical rate theory still needs to be quantified. Third, if the classical rate theory can reproduce observed swelling rates, what set of parameters, if any, give satisfactory results.

The outline of the paper is as follows. In Section 2, we briefly recapitulate classical rate theory for the purpose of introducing the basic parameters that enter the theory, and we discuss the ranges of acceptable values for them. In Section 3, we present the data which will be analyzed and some necessary details on the irradiation conditions. The results of our analysis are presented in Section 4. The significance of our findings will be evaluated in the final Section 5.

2. Classical rate theory

There are two kinds of reactions considered in the classical rate theory. First, the recombination or mutual recombination of interstitials and vacancies which belong to the freely migrating defect populations. This process of bulk recombination is derived as follows. We consider for the moment a vacancy as a sink for interstitials in a moving coordinate frame attached to the vacancy. In this moving frame, the relative migration coefficient is $(D_i + D_v)$, where D_i and D_v are the diffusion coefficient for the migration of interstitials and vacancies, respectively. The current of interstitials to a single vacancy is then given by

$$J_i^v = 4\pi R_c (D_i + D_v) C_i. \tag{1}$$

Here, C_i is the interstitial concentration in atomic fractions, and R_c is the recombination radius. It is the capture distance from the center of the vacant site, at which the interstitial is invariably drawn into the vacancy. For the determination of the recombination radius, the interaction forces between the annihilating pair must be known, and the diffusion equation in this force field must be solved. Schroeder [6] has provided a detailed review of this issue. Wolfer and Si-Ahmed [7] performed a numerical analysis for the recombination radius relevant to austenitic steels at temperatures in nuclear reactors. They showed that the recombination radius is expected to be from 2 to 3.5 times the lattice parameter. However, this was based on an interaction energy between vacancy and self-interstitial for an elastically isotropic material. Furthermore, the interaction was for the interstitial in its stable configuration rather than in its saddle-point position. For these reasons, we entertain in this study the possibility that the recombination radius could be as large as 7 times the lattice parameter, where the lattice parameter, $a0$, in the austenitic alloy is 3.639×10^{-10} m. To obtain from Eq. (1) the recombination rate, we multiply it with the number of vacancies per unit volume, which is C_v/Ω. Hence,

$$\text{Recombination rate (RR)} = \frac{4\pi R_c}{\Omega}(D_i + D_v) C_i C_v \tag{2}$$

in units of per second and per atomic site.

Next, the second kind of reactions are losses of point defects to sinks. The current of either vacancies or interstitials to a void of radius a is given by

$$J_{i,v}^0 = 4\pi a Z_{i,v}^0 D_{i,v} (C_{i,v} - C_{i,v}^0). \tag{3}$$

The subscripts i, v refer here and in following formulae to the *interstitials or vacancies*, while the superscript refers to the sink type. We will use the superscript 0 to indicate that the sink is a void. The current of point defects to other sink type can be written in the same form, namely

$$J_{i,v}^S = A^S Z_{i,v}^S D_{i,v} (C_{i,v} - C_{i,v}^S). \tag{4}$$

Here, A^S is a geometrical factor determined entirely by the dimensions and shape of the sink, $Z_{i,v}^S$ is the bias factor of the sink of type S for interstitials or vacancies, and $C_{i,v}^S$ is the concentration of interstitials or vacancies in local equilibrium with the sink. The second term in Eqs. (3) and (4) is the rate of thermal vacancy generation or re-emission by the sink. It should be noted that $C_i^S \approx 0$ for all sinks except perhaps very small interstitial clusters. Henceforth, this second term will be neglected for the interstitial currents J_i^S.

It is now a simple matter to set up the two basic equations of the classical rate theory. We denote by P the rate of displacements, and by ξ the fraction of vacancies and interstitials which escape the subsequent recombination in their native cascade. The defect fraction ξ can be inferred from resistivity changes in metals

irradiated to low doses at low temperatures, or it can be obtained from MD and kinetic MC simulations of cascades. A comprehensive review on this important parameter can be found in Averback and Diaz de la Rubia [8]. From these studies one finds that ξ depends strongly on the primary recoil energy, varying from a value of 0.7 for recoil energies just above the displacement energies to values as low as 0.1 for high-energy collision cascades. We employ values of 0.1 or 0.2 in this study, because the experiments were conducted in FFTF/MOTA, where fast neutrons produce the displacement damage in the form of collision cascades.

The basic assumption of classical rate theory is then that the average concentrations of vacancies and interstitials in a material subject to irradiation are determined by the two equations

$$\frac{\mathrm{d}C_\mathrm{v}}{\mathrm{d}t} = \xi P - \kappa D_\mathrm{v} C_\mathrm{v} D_\mathrm{i} C_\mathrm{i} - D_\mathrm{v} \sum_S N^S A^S Z_\mathrm{v}^S (C_\mathrm{v} - C_\mathrm{v}^S), \quad (5)$$

$$\frac{\mathrm{d}C_\mathrm{i}}{\mathrm{d}t} = \xi P - \kappa D_\mathrm{v} C_\mathrm{v} D_\mathrm{i} C_\mathrm{i} - D_\mathrm{i} \sum_S N^S A^S Z_\mathrm{i}^S C_\mathrm{i}, \quad (6)$$

where

$$\kappa = \frac{4\pi R_\mathrm{c}}{\Omega}\left(\frac{1}{D_\mathrm{v}} + \frac{1}{D_\mathrm{i}}\right) \quad (7)$$

is the recombination coefficient, and N^S is the density of sinks of type S per unit volume.

If the production rate P is constant, and if the geometrical factors A^S, the bias factors Z, and the sink densities N^S change over time scales much larger than the response times of vacancies and interstitials, then we may assume that a quasi-stationary state has been reached with $\mathrm{d}C_\mathrm{v}/\mathrm{d}t \approx \mathrm{d}C_\mathrm{i}/\mathrm{d}t \approx 0$. We can then solve the two rate equations for the steady-state defect concentrations and obtain

$$D_\mathrm{v} C_\mathrm{v} \approx \langle Z_\mathrm{i}\rangle \Psi + D_\mathrm{v}\langle C_\mathrm{v}^S\rangle, \quad (8)$$

$$D_\mathrm{i} C_\mathrm{i} \approx \langle Z_\mathrm{v}\rangle \Psi. \quad (9)$$

Here,

$$\Psi = \frac{\langle N\rangle}{2\kappa}\left\{\sqrt{\left[1 + \frac{\kappa D_\mathrm{v}\langle C_\mathrm{v}^S\rangle}{\langle Z_\mathrm{i}\rangle\langle N\rangle}\right]^2 + \frac{4\kappa\xi P}{\langle Z_\mathrm{i}\rangle\langle Z_\mathrm{v}\rangle\langle N\rangle^2}} - \left[1 + \frac{\kappa D_\mathrm{v}\langle C_\mathrm{v}^S\rangle}{\langle Z_\mathrm{i}\rangle\langle N\rangle}\right]\right\} \quad (10)$$

is the excess defect function,

$$\langle N\rangle = \sum_S A^S N^S \quad (11)$$

is the total sink strength,

$$\langle Z_\mathrm{i,v}\rangle = \frac{1}{\langle N\rangle}\sum_S A^S N^S Z_\mathrm{i,v}^S \quad (12)$$

are the average bias factors for interstitials and vacancies, respectively, and

$$\langle C_\mathrm{v}^S\rangle = \frac{1}{\langle Z_\mathrm{v}\rangle\langle N\rangle}\sum_S A^S N^S Z_\mathrm{v}^S C_\mathrm{v}^S \quad (13)$$

is the average thermal vacancy concentration in a material characterized by the various sinks present.

The net flow of defects into a particular sink of type Y is given by the difference in the interstitial and vacancy current, i.e. by

$$J_\mathrm{i}^Y - J_\mathrm{v}^Y = A^Y\{Z_\mathrm{i}^Y D_\mathrm{i} C_\mathrm{i} - Z_\mathrm{v}^Y D_\mathrm{v}(C_\mathrm{v} - C_\mathrm{v}^Y)\}.$$

If we insert the results from Eqs. (8) and (9) we obtain

$$J_\mathrm{i}^Y - J_\mathrm{v}^Y = A^Y Z_\mathrm{v}^Y\left\{\left[\frac{Z_\mathrm{i}^Y}{Z_\mathrm{v}^Y} - \frac{\langle Z_\mathrm{i}\rangle}{\langle Z_\mathrm{v}\rangle}\right]\langle Z_\mathrm{v}\rangle\Psi + D_\mathrm{v}[C_\mathrm{v}^Y - \langle C_\mathrm{v}^S\rangle]\right\}. \quad (14)$$

Eq. (14) can now be applied to any specific sinks, including voids.

According to Eq. (3), the geometric factor for a void of radius a is

$$A^0 = 4\pi a.$$

The equilibrium vacancy concentration for voids is given by

$$C_\mathrm{v}^0 = C_\mathrm{v}^\mathrm{eq}\exp\left\{\left(\frac{2\gamma}{a} - p_\mathrm{g}\right)\frac{\Omega}{kT}\right\}.$$

The net vacancy flux to the void is equal to the rate of growth of the void volume, which can be written with the general formula (14) as

$$4\pi a^2\frac{\mathrm{d}a}{\mathrm{d}t} = J_\mathrm{v}^0 - J_\mathrm{i}^0 = 4\pi a Z_\mathrm{v}^0\left\{\left[\frac{\langle Z_\mathrm{i}\rangle}{\langle Z_\mathrm{v}\rangle} - \frac{Z_\mathrm{i}^0}{Z_\mathrm{v}^0}\right]\langle Z_\mathrm{v}\rangle\Psi - D_\mathrm{v}[C_\mathrm{v}^0 - \langle C_\mathrm{v}^S\rangle]\right\}. \quad (15)$$

This equation for void growth contains two terms. The first term which is proportional to Ψ is the bias-driven or radiation-driven term, while the second one is the annealing term. This last term is proportional to

$$D_\mathrm{v}[C_\mathrm{v}^0 - \langle C_\mathrm{v}^S\rangle] \propto D_\mathrm{v} C_\mathrm{v}^\mathrm{eq},$$

i.e. of the order of the self-diffusion coefficient.

The annealing term opposes void growth when $C_v^0 > \langle C_v^S \rangle$. Since the average equilibrium vacancy concentration $\langle C_v^S \rangle$ is dominated by dislocations, and since $C_v^{disl} \approx C_v^{eq}$, we may use the following approximation:

$$D_v[C_v^0 - \langle C_v^S \rangle] \approx D_v C_v^{eq} \left[\exp\left\{ \left(\frac{2\gamma}{a} - p_g \right) \frac{\Omega}{kT} \right\} - 1 \right].$$

We see that this term is positive when the surface tension is greater than the gas pressure in the void, i.e. when $2\gamma/a > p_g$.

At temperatures below 550 °C, this annealing term is negligible. The condition for void growth is then that the so-called net bias must be positive, i.e.

$$B = \frac{\langle Z_i \rangle}{\langle Z_v \rangle} - \frac{Z_i^0}{Z_v^0} > 0. \tag{16}$$

Sniegowski and Wolfer [9] have developed sets of bias factors for edge dislocations, prismatic loops, and for voids. The last two sets are found to depend strongly on the loop and the void radius, respectively. The bias factors for dislocations, on the other hand, must be averaged over different configurations, taking into account edge and screw characters and the mutual cancellation of the long-range stress fields when dislocations form multipole configurations [10] or walls. For all these reasons, the net bias evolves with the microstructure. When dislocation loops and voids attain radii of about 3 nm or larger, the net bias becomes dominated by the dislocation network and approaches a limiting value. Sniegowski and Wolfer [9] have shown that this limiting value determines the steady-state void swelling rate. In the case of austenitic steels, the final swelling rate of about 1%/dpa is consistent with a defect fraction of $\xi = 0.1$ and a bias factor ratio for dislocations of $Z_i^{dis}/Z_v^{dis} \cong 2$, indicating a microstructure composed mainly of dislocations with edge character. Accordingly, we select $Z_i^{dis}/Z_v^{dis} \cong 2$ as the upper value for the range of possible bias factor ratios. Traditionally, however, smaller values have been used by other researchers. Tenbrink et al. [11] have attempted to extract the net bias for void swelling in AISI 316 L under dual ion irradiation by fitting the growth rate of large voids to the rate theory. The net bias B was found to vary between 0.1 and 0.45 at a dose of 9.1 dpa with the highest value for lower dose rates of 10^{-4} dpa/s and the low value for 10^{-2} dpa/s. However, when Tenbrink et al. assumed neutral voids, having bias factors of one, dislocation bias factors as high as 3 were inferred. For the present study, we select then a range of values for Z_i^{dis}/Z_v^{dis} from 1.1 to 2.0. On the other hand, since most of the voids observed in this experiment are larger than 3 nm, as we will show in the next section, they can be considered as neutral sinks, and the void bias factors can be set to 1.0.

Void growth rate in the bias-dominated temperature range depends critically on the excess defect function Ψ. This function diminishes with decrease in irradiation temperature. This is due to the fact that vacancy mobility decreases, thereby enhancing the vacancy concentration C_v and the recombination rate with interstitials. Recombination is therefore controlled by the vacancy migration rather than the interstitial migration. This curious fact can be explained easily by examining the recombination coefficient κ as defined in Eq. (7). When $D_i \gg D_v$, a good approximation is

$$\kappa \approx \frac{4\pi R_c}{\Omega D_v}$$

and the function Ψ becomes dependent only on D_v. At low temperatures, where $4\xi P\kappa/\langle N \rangle^2 \gg 1$,

$$\Psi \approx \sqrt{\xi P/\kappa} \propto \sqrt{\xi P D_v}$$

and the void growth rate is then proportional to the square root of the dose rate. Therefore, the choice of the vacancy migration is one of the crucial parameters in the classical rate theory. D_v is written in the usual form as

$$D_v = D_{v0} \cdot \exp\left(-\frac{E_v}{kT} \right).$$

Here D_{v0} is the pre-exponential factor, and it will be set equal to 1.286×10^{-6} m^2/s, k is the Boltzmann constant, and T is the temperature in degree Kelvin. Although there exists uncertainty about D_{v0}, this is masked by the uncertainty in the activation energy E_v. There are some experimental results reported in the literature. For example, Dimitrov and Dimitrov [12] found a value of 1.28 ± 0.17 eV from electrical resistivity measurements of neutron-irradiated Fe–16Cr–20Ni and Fe–16Cr–25Ni containing minor elements. Other experiments conducted by Kuramoto et al. [13] yielded a migration energy of 1.36 eV as extracted from positron annihilation measurements of electron-irradiated 316 SS and JPCA. Based on these experiments, we consider activation energies of 1.2, 1.3 and 1.4 eV.

For high temperatures, $T > 550$ °C, $4\xi P\kappa/\langle N \rangle^2 \ll 1$, and $\Psi \propto \xi P$. The void growth rate becomes now proportional to the dose rate.

Eq. (15) gives the growth rate of a particular void at the time when its radius is a. In a material that has been exposed to irradiation for some time, the actual voids have a distribution in size. Our TEM observations on irradiated materials provide this void size distribution in the form of histograms, giving the number N_h of voids per unit volume with radii in the interval $(a_h - \Delta a/2)$ and $(a_h + \Delta a/2)$. Assuming that within a short time interval dt the void number densities do not change, the void swelling rate can be computed with

$$\frac{\mathrm{d}\left(\frac{\Delta V}{V}\right)}{\mathrm{d}t} = \sum_h N_h^0 4\pi a_h^2 \frac{\mathrm{d}a_h}{\mathrm{d}t} = \sum_h 4\pi a_h N_h^0 Z_v^0(a_h) \times \left\{ \left[\frac{\langle Z_i \rangle}{\langle Z_v \rangle} - \frac{Z_i^0(a_h)}{Z_v^0(a_h)} \right] \langle Z_v \rangle \Psi - D_v [C_v^0 - \langle C_v^S(a_h) \rangle] \right\}. \quad (17)$$

Eq. (17) is evaluated in the following Section 4 using measured sink densities and different combinations of parameter values in their selected ranges.

3. Experimental microstructure data

The materials considered in the present study are solution-annealed Fe–15Cr–16Ni ternary alloys, made from high purity Fe, Cr and Ni without any other minor elements. TEM samples were placed at seven different positions in a FFTF/MOTA assembly within, below, and above the core. An important feature of this irradiation was a variation of more than two orders in dose rate, but a very narrow range of irradiation temperatures. The FFTF/MOTA assembly has an active and precise temperature-control system. All temperatures were kept between 408 and 444 °C, independent of dose rate, with one exception at 387 °C [14,15]. The first irradiation sequence occurred in Cycle 11 of FFTF operation in MOTA-2A, after which a subset of specimens were removed. The other identical specimens continued irradiation in Cycle 12 in MOTA-2B assembly. Table 1 summarizes the irradiation conditions for both cycles. After irradiations, the immersion density technique was used to determine the swelling, followed by TEM (transmission electron microscopy) observations of the specimens.

Microstructural examination revealed that voids, faulted dislocation loops, and perfect dislocation loops and finally network dislocations were the only microstructural features observed. There were no pre-existing or radiation-induced precipitates observed in any samples, as expected.

Fig. 1 shows the swelling for the highest five dose rates as a function of cumulative dose. These swelling data come from TEM observation below 10% swelling, and from immersion density measurement above 10% swelling. When more than one specimen was measured by immersion density, the swelling was remarkably consistent between specimens. Lower dose rates yielded higher swelling by shortening the incubation dose for the onset of steady-state swelling. It is also very significant that the steady-state swelling rate of 1%/dpa is not affected by the dose rate, as is also observed in similar austenitic alloys irradiated at a fixed dose rate in the EBR-II fast reactor [16,17], or in commercial austenitic stainless steels irradiated in a variety of reactors [18–20].

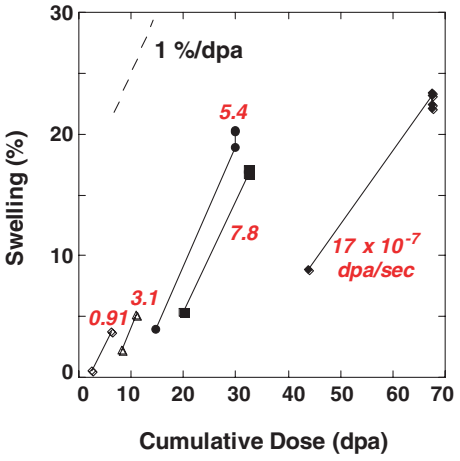

Fig. 1. Swelling in Fe–15Cr–16Ni irradiated in FFTF/MOTA as a function of cumulative dose and for the dose rates indicated.

Table 1
Irradiation conditions for specimens

Dose rate (dpa/s)		Dose (dpa)		Temperature (°C)	
#11	#12	#11	#11 and #12	#11	#12
1.7×10^{-6}	1.4×10^{-6}	43.8	67.8	427	408
7.8×10^{-7}[a]	9.5×10^{-7}	20.0[a]	32.4	390	387
5.4×10^{-7}	8.4×10^{-7}	14.0	28.8	430	424
3.1×10^{-7}[b]	3.0×10^{-7}	8.05[b]	11.1	411	410
9.1×10^{-8}	2.1×10^{-7}	2.36	6.36	430	431
2.7×10^{-8}	6.6×10^{-8}	0.71	1.87	434	437
8.9×10^{-9}	2.2×10^{-8}	0.23	0.61	436	444

[a] 6.0×10^{-7} dpa/s and 15.6 dpa for 2 cycle irradiation specimens.
[b] 2.2×10^{-7} dpa/s and 5.69 dpa for 2 cycle irradiation specimens.

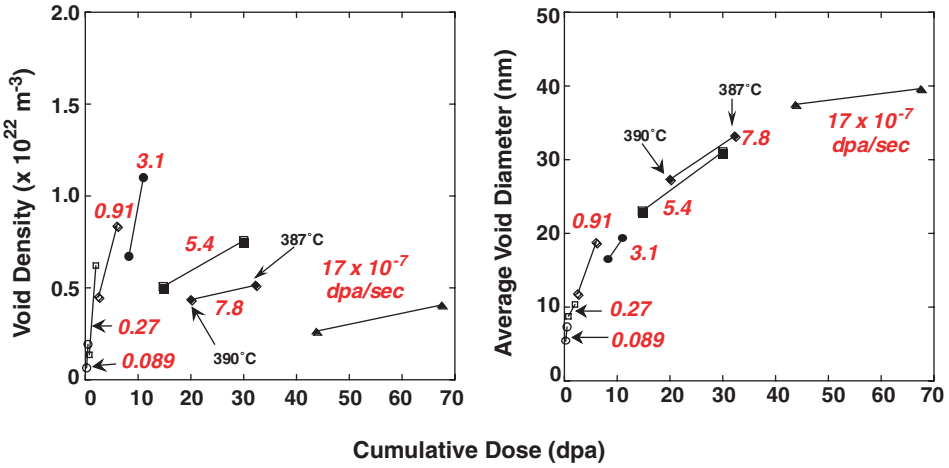

Fig. 2. Void density and average diameters as a function of cumulative dose and for the dose rates indicated.

It should be emphasized again, that the dose levels achieved in this study appear to be above the incubation dose, and steady-state swelling has already been reached.

Fig. 2 shows the void density and average diameter over the wide range of dose rates as a function of cumulative dose. Note that the helium generation rates per dpa in all the irradiation conditions are rather low, i.e. helium varies between 0.07 and 0.3 appm/dpa [21]. At a fixed dose rate, the void density increases with dose. However, both the absolute value and the rate of increase in void density are higher at low dose rates, indicating more voids are nucleated at lower dose rates. Average void diameter, on the other hand, appears to be only a function of cumulative dose and independent of dose rate.

Fig. 3 shows the total dislocation density for all seven different dose rates as a function of cumulative dose.

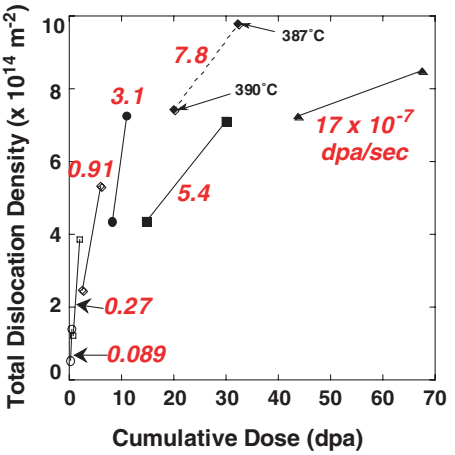

Fig. 3. Total dislocation density as a function of cumulative dose and for the dose rates indicated.

Lower dose rates enhance dislocation evolution. This effect arises primarily from the enhanced formation of dislocation loops at lower dose rate.

The void density, its average diameters, loop line length and network dislocation density observed in each irradiation condition are listed in Table 2. Table 2 also shows the void sink strengths, calculated as $4\pi r_c \cdot N_c$ and used as input in the following calculations. Here, r_c and N_c denote the average void radius and void density, respectively.

4. Predicted swelling rates

With the selected ranges of acceptable values for the basic parameters, a list of 72 different combinations were chosen and swelling rates predicted for the two doses achieved in the experiments. From these combinations, we can identify 9 which produce swelling rates in reasonable agreement with the experimental results. Table 3 denotes the possible 9 parameter sets that give the swelling rates most agreeable with the experimental results. To be more specific, we judge the predictions to agree with the observed swelling trends when the swelling rates for each irradiation condition at the two corresponding doses line up with each other and with the line connecting the two experimental values of swelling. This line-up has to be satisfactory for each pair.

It is surprising that swelling rate calculations based on the classical rate theories agree so well with the experimental results when parameter values are chosen that are derived from other experimental and theoretical sources.

It is also found that the sensitivity to variation in one parameter depends on other parameters. For example, the difference of parameter sets #2 and #3 is only in the

Table 2
Microstructure parameters for specimens

Irradiation condition		Void			Dislocation density (m^{-2})		
dpa/s in MOTA-2A	Dpa	Density (m^{-3})	Average diameter (nm)	Sink strength (m^{-2})	Loops	Network	Total
8.9×10^{-9}	0.23	6.5×10^{20}	5.4	2.2×10^{13}	1.9×10^{13}	3.5×10^{13}	5.4×10^{13}
	0.61	1.9×10^{21}	7.4	8.8×10^{13}	2.8×10^{13}	1.1×10^{14}	1.4×10^{14}
2.7×10^{-8}	0.71	1.4×10^{21}	8.7	7.6×10^{13}	4.9×10^{13}	7.4×10^{13}	1.2×10^{14}
	1.87	6.2×10^{21}	10.3	4.0×10^{14}	1.0×10^{14}	2.9×10^{14}	3.9×10^{14}
9.1×10^{-8}	2.36	4.5×10^{21}	11.8	3.3×10^{14}	9.4×10^{13}	1.5×10^{14}	2.5×10^{14}
	6.36	8.4×10^{21}	18.7	9.9×10^{14}	2.0×10^{14}	3.4×10^{14}	5.4×10^{14}
3.1×10^{-7}	8.05	6.7×10^{21}	16.7	7.0×10^{14}	2.5×10^{14}	1.9×10^{14}	4.4×10^{14}
2.2×10^{-7}	11.1	1.1×10^{22}	19.3	1.3×10^{15}	2.9×10^{14}	4.4×10^{14}	7.3×10^{14}
5.4×10^{-7}	14.0	5.1×10^{21}	23.1	7.4×10^{14}	2.2×10^{14}	2.1×10^{14}	4.3×10^{14}
	28.8	7.6×10^{21}	31.1	1.5×10^{15}	–	7.1×10^{14}	7.1×10^{14}
7.8×10^{-7}	20.0	4.3×10^{21}	27.4	7.4×10^{14}	–	7.4×10^{14}	7.4×10^{14}
6.0×10^{-7}	32.4	5.2×10^{21}	33.2	1.1×10^{15}	–	9.8×10^{14}	9.8×10^{14}
1.7×10^{-6}	43.8	2.6×10^{21}	37.5	6.1×10^{14}	–	7.3×10^{14}	7.3×10^{14}
	67.8	4.1×10^{21}	39.6	1.0×10^{15}	–	8.5×10^{14}	8.5×10^{14}

Table 3
Acceptable combinations of parameter values

	Recombination radius, r_c	Dislocation bias factor		Vacancy migration energy (eV)	Cascade efficiency
		Loops (Zl)	Networks (Zd)		
#1	2.0a0	1.40	1.25	1.4	0.2
#2	2.0a0	1.55	1.40	1.3	0.1
#3	2.0a0	1.55	1.40	1.4	0.1
#4	3.5a0	1.40	1.25	1.4	0.2
#5	3.5a0	1.55	1.40	1.2	0.1
#6	3.5a0	1.55	1.40	1.3	0.1
#7	7.0a0	1.40	1.25	1.3	0.2
#8	7.0a0	1.55	1.40	1.3	0.1
#9	7.0a0	1.55	1.40	1.4	0.2

migration energy for vacancies, indicating that for the particular choice of the other parameters, the swelling rate is insensitive to E_v. However, parameter combinations containing the smallest values for the biases of dislocation loops and network dislocations result always in low swelling rates although other parameters are chosen to obtain the largest possible swelling rate. Hence, dislocation bias factor ratios of 1.1 are clearly too small and not compatible with the present experimental results. It is also found that the bias factor ratios of 2.0 are too large even when other parameters are chosen such that the smallest possible swelling rate is predicted.

Fig. 4 shows the calculated swelling rate at seven different dose rates with the 9 acceptable parameter sets described in Table 3. Fig. 4 also shows the experimental results. Over the wide range of dose rates, the calculated swelling rate appears to be in good agreement with the experimental results. Unfortunately, in this study, it is impossible to specify one best parameter set. However, it is demonstrated that the classical rate theory works surprisingly well with sets of parameters that fall within reasonable ranges of uncertainty.

Nevertheless, for each of the nine best parameter sets, a minor, but consistent difference can be observed between the swelling rates at the lower and at the higher dose rates. The latter are always somewhat larger than the former. In contrast, the experimental swelling rate at the highest dose rate is noticeably smaller than that at lower dose rate. However, this minor disagreement is insufficient to declare classical rate theory deficient or invalid.

5. Discussion and conclusions

From the results presented in the previous section, it can be concluded that the classical rate theory is able to

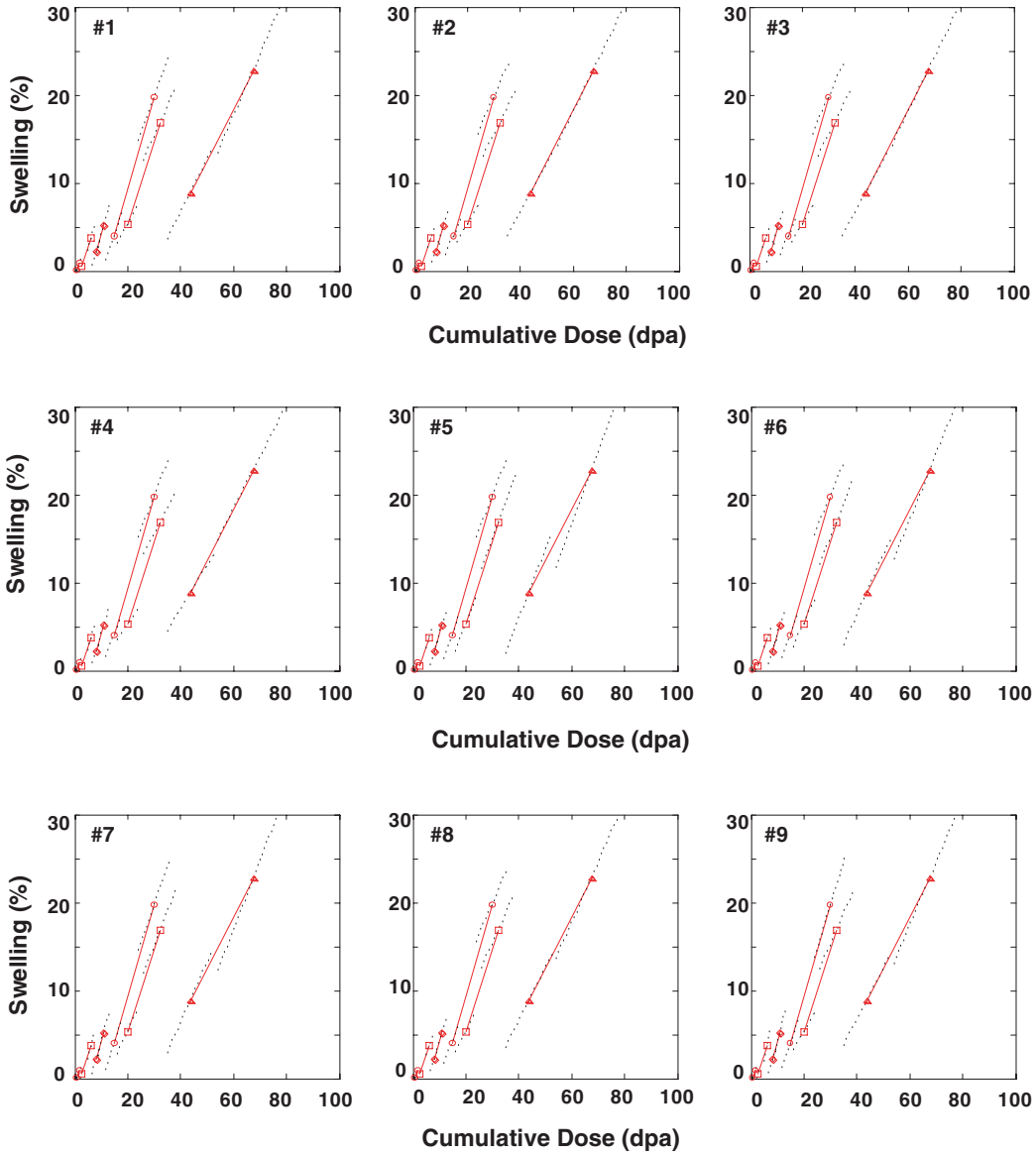

Fig. 4. Comparison between the swelling rates obtained from rate theory (dotted lines) and the experimental results. Pairs of experimental data for the same irradiation condition but two different doses are connected by a solid line. The number associated with each plot corresponds to the parameter set listed in Table 3.

predict void swelling with parameter values that have a sound basis. Even though it consists of only two equations, many other phenomena identified more recently can apparently be neglected. A major difference between the classical rate theory and modern atomistic simulations, such as MD or kinetic MC, is the realization that numerous small defect clusters are generated initially in cascades and are highly mobile at irradiation temperatures. These findings are summarized in Refs. [22,23]. It has also been verified experimentally [24,25] that these clusters are mobile and can strongly affect the subsequent microstructural evolution. However, this study appears to suggest that it is not necessary to add more equations for these clusters in order to predict the swelling rate. As we show in Appendix A, it is possible to combine all rate equations for mobile interstitial clusters into one for an apparent or effective self-interstitial concentration, and that this one equation has the same form as in the classical rate theory, provided all mobile interstitial clusters have diffusivities much greater than vacancies. Furthermore, the direct production of interstitial clusters in cascades does not create

a production bias if these clusters are mobile, and are absorbed at the sinks.

The experimental results of the swelling rate at the highest and lowest dose rates are lower than 1%/dpa. This is probably because the steady-state swelling has not been reached at the lowest dose rate and dose, nor at the highest dose rate because of the long incubation dose at high dose rates. Unfortunately, the classical rate theory cannot explain such a strong effect of dose rate on the incubation dose for the swelling. Such a pronounced dose rate effect is probably due to void nucleation being dependent separately on time and dose rate. In addition, the evolution of dislocation loops and network dislocations also exhibit a strong dose rate dependence [5,14,26].

We measured in our experiments only the densities and sizes of visible clusters. However, there may also be a significant amount of invisible, small clusters, which may contribute to the sink densities. In the present set of data, it appears that the radiation dose is beyond the void nucleation phase, and that for the void growth phase, these invisible clusters play only a minor role.

For future modeling work, however, it is important to explore the effect of invisible cluster, as they affect the incubation period of void swelling. Since the rate theory for void swelling gives satisfactory results, the important tasks for future work will be the development of comprehensive microstructural evolution models.

Acknowledgements

The authors gratefully acknowledge support of this work by a NERI grant from the US Department of Energy under contract W-7405-ENG-48 with the Lawrence Livermore National Laboratory.

Appendix A. An effective rate equation for interstitials

Numerous atomistic computer simulations of collision cascade have provided evidence that interstitials aggregate in their native cascades into small clusters. These clusters are highly mobile at irradiation temperatures in nuclear reactors, and as a result, each cluster size should be described by a rate equation.

Let us therefore denote the concentration of interstitial clusters with n atoms by I_n, and their rate of production in cascades by P_n. Although some vacancies also form clusters within cascades, these clusters dissolve rather than migrate as entities. Hence, we need to consider only mono-vacancies as mobile.

For extremely low sink densities, as may be the case in the very early stage of an irradiation, interstitial clusters may coalesce and form dislocation loops. However, during later stages when the sink densities are higher, interstitial clusters will most likely be absorbed at sinks rather than react with other interstitial clusters in transit. Accordingly, the rate equations for interstitial clusters may be written as,

$$\frac{\mathrm{d}I_n}{\mathrm{d}t} = P_n - R_n^{IV} \cdot I_n \cdot V + R_{n+1}^{IV} \cdot I_{n+1} \cdot V - L_n^I \cdot I_n \cdot S. \tag{A.1}$$

Here, R_n^{IV} is the recombination rate coefficient for vacancies with interstitial cluster I_n, and L_n^I is the rate of absorption of these clusters at all the sinks with a total strength of S. Both R_n^{IV} and L_n^I are proportional to the diffusion coefficient D_n^I of the interstitial clusters of size n, and no assumption needs to be made on the mode of diffusion. We note that

$$\langle P \rangle = \sum_n n \cdot P_n \tag{A.2}$$

is the total rate of interstitial production, and it is equal to the total rate of vacancy production by displacements. Furthermore, the total interstitial concentration in transit is

$$\langle I \rangle = \sum_n n \cdot I_n. \tag{A.3}$$

If we multiply Eq. (A.1) by n and sum over n, we obtain after a few simple manipulations

$$\frac{\mathrm{d}\langle I \rangle}{\mathrm{d}t} = \langle P \rangle - \langle R \rangle \cdot \langle I \rangle \cdot V - \langle L \rangle \cdot \langle I \rangle \cdot S, \tag{A.4}$$

where

$$\langle R \rangle = \left(\sum_n R_n^{IV} \cdot I_n \right) \Big/ \langle I \rangle \tag{A.5}$$

is an average recombination coefficient and

$$\langle L \rangle = \left(\sum_n L_n \cdot n \cdot I_n \right) \Big/ \langle I \rangle \tag{A.6}$$

an average loss rate coefficient at sinks.

Eq. (A.4) has the same form as the rate equation for mono-interstitials used in classical rate theory.

Therefore, we may simply view the latter as the average rate equation (A.4) for all mobile interstitials. As long as the vacancy diffusion coefficient is the lowest, interstitial mobilities have no impact on the void growth rate, and it does not matter if interstitials arrive at sinks as clusters or as mono-defects.

References

[1] S.D. Harkness, C.Y. Li, in: J.W. Corbett, L.C. Ianniello (Eds.), Proc. of the International Conference on Radiation-Induced Voids in Metals, 1971, p. 798.

[2] A.D. Brailsford, R. Bullough, J. Nucl. Mater. 44 (1972) 121.
[3] H. Wiedersich, Radiat. Eff. 12 (1972) 111.
[4] F.A. Garner, in: R.W. Cahn, P. Haasen, E.J. Kramer (Eds.), Chapter 6 in Materials Science and Technology, vol. 10A, VCH Publisher, Weinheim, 1994, p. 419.
[5] T. Okita, N. Sekimura, F.A. Garner, L.R. Greenwood, W.G. Wolfer, Y. Isobe, in: Proc. of the 10th International Symposium on Environmental Degradation of Materials in Nuclear Power Systems–Water Reactors, 2001, on CD.
[6] K. Schroeder, in: Point Defects in Metals II, Springer-Verlag, Berlin, 1980.
[7] W.G. Wolfer, A. Si-Ahmed, J. Nucl. Mater. 99 (1981) 117.
[8] R.S. Averback, T. Diaz de la Rubia, in: H. Ehrenreich, F. Spaepen (Eds.), Solid State Physics, vol. 51, Academic Press, 1998, p. 281.
[9] J.J. Sniegowski, W.G. Wolfer, in: Proc. of Topical Conference on Ferritic Alloys for Use in Nuclear Energy Technologies, Snowbird, Utah, 19–23 June 1983.
[10] W.G. Wolfer, M. Ashkin, A. Boltax, ASTM-STP 570 (1975) 233.
[11] J. Tenbrink, R.P. Wahi, H. Wollenberger, J. Nucl. Mater. 155–157 (1988) 850.
[12] O. Dimitrov, C. Dimitrov, J. Nucl. Mater. 105 (1982) 39.
[13] E. Kuramoto, N. Tsukada, Y. Aono, M. Takenaka, Y. Takano, H. Yoshida, K. Shiraishi, J. Nucl. Mater. 133&134 (1985) 561.
[14] T. Okita, T. Sato, N. Sekimura, F.A. Garner, L.R. Greenwood, J. Nucl. Mater. 307–311 (2002) 322.
[15] L.R. Greenwood, L.S. Kellogg, DOE/ER-0313/12 (1992) 49.
[16] F.A. Garner, H.R. Brager, ASTM-STP 870 (1985) 187.
[17] F.A. Garner, A.S. Kumar, ASTM-STP 955 (1987) 289.
[18] F.A. Garner, L.R. Greenwood, D.L. Harrod, in: Proc. of the 6th International Symposium on Environmental Degradation of Materials in Nuclear Power Systems Water Reactors, 1993, p. 783.
[19] F.A. Garner, J. Nucl. Mater. 122&123 (1984) 459.
[20] F.A. Garner, J. Nucl. Mater. 205 (1993) 98.
[21] T. Okita, W.G. Wolfer, F.A. Garner, N. Sekimura, to be published in J. Nucl. Mater.
[22] D.J. Bacon, F. Gao, Y.N. Osetsky, J. Nucl. Mater. 276 (2000) 1.
[23] Y.N. Osetsky, D.J. Bacon, A. Serra, B.N. Singh, S.I. Goulubov, J. Nucl. Mater. 276 (2000) 65.
[24] M. Kiritani, J. Nucl. Mater. 276 (2000) 41.
[25] H. Abe, N. Sekimura, Y. Yang, J. Nucl. Mater. 323 (2003) 220.
[26] T. Okita, T. Kamada, N. Sekimura, J. Nucl. Mater. 283–287 (2000) 220.